INTERNATIONAL JOURNAL of RENEWABLE ENERGY RESEARCH
S.Q.Hussien and A. A. Farhan, Vol.9, No.2, June, 2019

The Effect of Metal Foam Fins on the Thermo-hydraulic Performance of a Solar Air Heater

Sally Qussay Hussien *, Ammar A. Farhan*[‡]

*Department of Energy Engineering, College of Engineering, University of Baghdad, Baghdad, Iraq.

(sallyqussay@gmail.com, ammarali@uobaghdad.edu.iq)

[‡] Corresponding Author; Ammar A. Farhan, Tel: +964 7712901111, ammarali@uobaghdad.edu.iq

Received: 14.03.2019 Accepted:22.04.2019

Abstract- The metal foam porosity helps the air to penetrate through the fins and extracted more heat gain from the absorber plate. In this experimental study, the effect of metallic foam fins on the thermohydraulic efficiency is investigated through a test rig built for this purpose. Fins with different metal foam pore density (PPI), and three different configurations (longitudinal, corrugated, and staggered) are attached to the back surface of the absorber plate. The experiments are conducted under Baghdad climatic conditions for February, March and April 2018. The results showed that the presence of metal foam fins provided a large surface area for convective heat transfer so that, the air temperature difference and thermal efficiency of the solar collector are increased. The maximum temperature difference for corrugated, staggered, longitudinal metallic foam, and solid longitudinal fins at an air flow rate of 0.01 m^3/s is 31, 27, 23, and 17 ℃, respectively. Metal foam fins with higher PPI exhibited higher air temperature difference due to higher heat transfer surface area. The highest value of the thermal and effectiveness efficiencies for corrugated metal foam fins are 86 %, and 79 %, respectively.

Keywords solar air heater, metal foam, metal foam fins, performance analysis, thermohydraulic efficiency

1. Introduction

Solar energy coming from the Sun and collected by a solar collector (SC) represents an alternative way to minimize the dependency on the non-conventional energy sources in Iraq. Thereby, the greenhouse effects, harsh summer weather, and global warming potential are reduced to make life safer. More than 290 sunny days are available in Iraq with solar radiation around 1000 W/m^2 at noon. Solar air heaters (SAHs) are devices that have been constructed to exploit this energy.

SAH consists in its simplest way of absorber plate that absorbs the solar radiation that hits the upper surface and a working fluid (Air) flowing over/below the absorber surface to carry the absorbed heat. The upper side of the SAH is made of transparent material (glass) which allows the solar radiation to pass through it, whereas the bottom and the sides of SAH are typically insulated to reduce heat losses. SAH has low thermal performance which represents a significant disadvantage of these collectors due to the low specific heat of air [1-3]. Different techniques and modifications were adopted to enhance the heat transfer between the air and the absorber surface such as using fins to impose turbulence flow inside the fluid duct [4-6] or use a perforated surface to provide a larger area for the heat transfer process [7]. The effects of fins and baffles on the thermal efficiency of SAH has been studied theoretically and experimentally [8]. Different ranges of mass flow and fin parameters like; fin width and spacing were used. Results show that adding fins and baffles improve the thermal efficiency of the SC whereas, increasing the fins and baffles required a high pump work which led to reduce the effective efficiency. Also, the optimum fins and baffles parameters for this work were estimated for each range of mass flow rates.

Fins attached to internally recycled SAHs were studied theoretically by Ref. [9]. It was shown that the improvement in the collector efficiency was over 100% with the recycling operation**.** The influence of adding rectangular fins on the temperature difference across the SC has been investigated experimentally [10]. The absorber plate was tested with selective and non-selective material. The obtained results were compared with the results of SAH with no fins attached; this illustrates that attaching fins will enhance the performance of the SC, while the selectivity of the absorber surface showed no significant difference in the presence of fins.

The effect of adding porous material in the lower channel of the double pass SAH was examined experimentally and theoretically [11]. A comparison between double pass SC with and without pours material was held. This study showed that adding the porous material provided a higher outlet temperature as compared to traditional double pass SC thereby; an enhancement in thermal efficiency was obtained. An analytical examination on the performance of corrugated herringbone fins that are located below the absorber surface has been conducted [12]. MTLAB software was used to solve the energy balance equation of the system, taking into consideration the variation of the air flow rate, fin pitch, and fin spacing. The result showed enchantment of 20.4% to the efficiency of the collector when the herringbone fins are added. The efficiency of finned absorber plate of double pass SAH with two inlet ports was implemented experimentally [13]. The absorber plate used in this experiment has four different configurations; conventional flat plate, a plate with pin fins, a plate with corrugated fins, and plate with corrugated-perforated fins. Different percentages of the air flow rate entering the collector were adopted for all four plate configurations. The result obtained showed that the efficiency of perforated-corrugated fins was the largest while the flat absorber plate showed the lowest efficiency. In order of the percentage of flowing air, the result showed that increasing the flowing air in the upper port reduces the temperature of the absorber plate and enhances the performance of SAH for all absorber plate configurations. solar energy availability has coincided with the demand of the air-conditioning applications [14-15].

Metal foam is cellular structures that have a solid matrix of metal, containing a large volume fraction of fluid-filled pores. The pores can be sealed (closed cell metal foam), or consist of ligaments forming an interconnected network (open cell metal foam) [16]. Metal foam exhibit different attractive characteristics when compared to their solid material counterparts. It is used for engineering and medical applications. Foams and other porous materials have a cellular structure known to have great engaging combinations of physical and mechanical properties, such as high thermal conductivity, high fluid permeability, and high stiffness in conjunction with very low weight. Therefore, nature often uses cellular materials for various functional or constructional purposes. Metallic foams are made out of different types of materials including copper, Aluminum, Nickel or Titanium. The application type of metallic foams eventually decides the kind of material is made off. Open cell metal foams are permeable and can possess high specific surface areas and special features essential for flow-through applications or when the surface exchange is involved. Metal foam enhance heat transfer rate by increasing the contact surface area between the absorber plate and the working fluid, and provide better mixing between them [11]. The thermal performance of a SC was improved by inserting metal foam in the paraffin. Also, it was found that, the temperature distribution was more uniformly inside the paraffin with metal foam as compared with paraffin without metal foam [17]. SAH with absorber plate made from porous and non-porous material was investigated experimentally [18]. Results show that, the SAH efficiency was 61 % at solar noon. A review paper discussed the application of porous material including metal foam in solar energy system presented by Ref. [19].

In this study, the main objective is to investigate the thermos-hydraulic performance of SAH with metal foam fins attached to the lower surface of the absorber plate. Copper metal open cell foam fins of 15 and 20 PPI with different configurations have been studied. Fin configurations are; (i) longitudinal fins, (ii) corrugated fins, (iii) staggered fins.

2. Experimental Work

An experimental set-up was manufactured to study the performance of the SC with metal foam fins. Two outdoor solar collectors with single glass cover were constructed and installed as reported in ASHRAE recommendations. First SAHs was constructed with solid longitudinal fins (1mm thickness) and the other with the open cell metal foam fins (5 mm thickness) for the sake of comparison between the two SAHs performance. The SAHs were built from common materials in the local market. The test rigs consisted of a centrifugal blower, single glass sheet, absorber plate, fins attached to the lower surface of the absorber plate. Thermal losses from the bottom and sides of the SC were reduced by thermal insulation with a thickness of 5 and 2.5 cm, respectively. A Wooden frame collected these components as shown in Fig. 1. The two collectors had the same dimensions 100 cm in length × 90 cm in width × 22.5 cm in height. An ordinary glass of 4 mm thickness covers the SC. Silicon tape was used to seal the cover edges to prevent hot air from leakage to outside the SC. The absorber plates were made of galvanized steel of 1 mm thickness. A schematic diagram for the cross-sectional area of the SAH was shown in Fig. 2.

Fig.1. Photograph of the experimental test rigs.

Three fin configurations which attached to the absorber plate were investigated. First, longitudinal metal foam fins (Fig. 3, a) arranged uniformly in rows in the flow directions. Fins height is 50 mm and the 5 mm thickness. Second, corrugated metal foam fins (Fig. 3, b) with an inclination angle of 30^{o}.The third configuration is staggered metal foam fins (Fig. 3, c) in the same direction of the air flow. A photograph for the metal foam fins installed inside the SAH was shown in Fig. 3d. The equal lateral distance between each consecutive fins was made. For all cases, the fins are attached to the lower surface of the absorber plate. The absorber plate surfaces were painted with matte black paint for absorbing maximum portion of the sun's radiation.

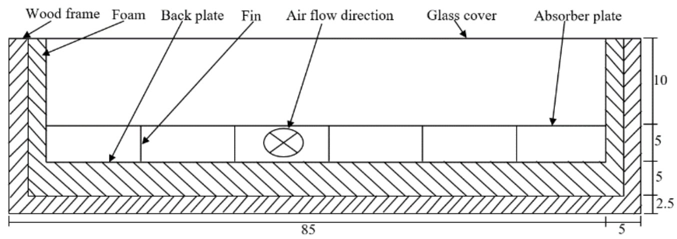

Fig. 2. Schematic diagram for the cross-sectional area of the SAH. All dimensions in centimeters.

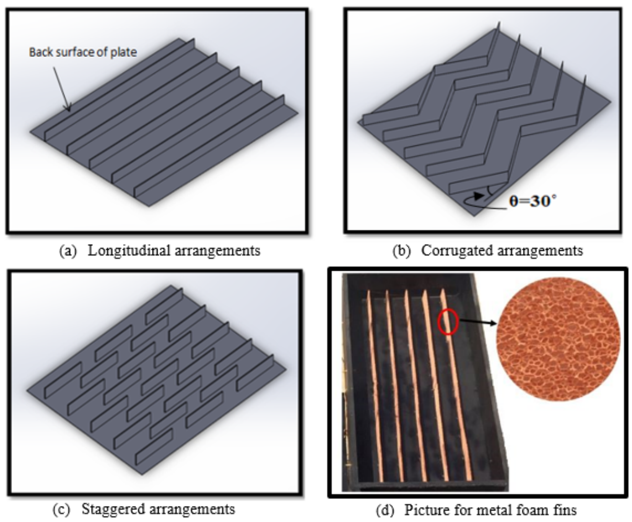

Fig. 3. Schematic diagram for fin arrangements.

The experiments were implemented during February, March, and April 2018. The test rigs were operated under the weather condition of Baghdad (33 ^{o}N, 44 ^{o}E). The SAH is assembled on an inclined frame having an inclination angle of 43^{o} and is oriented to the south during all experiments to receive the maximum solar radiation. The SAH body is supported on a metal stand. Solar radiation d ata was taken from the Iraqi meteorological station in the Ministry of Science and Technology for the testing days. Temperature is a vital indicator of the energy obtained from SC, which determines the efficiency of the system. Therefore, arrays of thermocouples were used to determine the temperature distribution within the body of the SC. Eight thermocouples type K were used to record temperature every 30 minutes for each SAH. Six thermocouples were fixed on the absorber plate at an equal distance, i.e., three thermocouples in the longitudinal direction and three in the transverse direction. Two thermocouples were used to measure the inlet and outlet air. The ambient temperature was recorded by a thermocouple shielded from the direct solar radiation. The air flow rates were measured by using a multi-function measuring instrument. The experimental period was from 9 AM till 4 PM. Five values of air flow rates were handled ranging between 0.01 – 0.05 m^3/s.

3. Thermal Analysis

In steady state, the conversion of absorbed solar energy into useful energy gain and thermal losses is governed by energy balances equation which indicates the performance of the SAH. The absorbed energy is the amount of solar energy hits the upper black surface of the SAH and absorbed by the absorber plate is given by [20]

$$Q_i = IA_c \tag{1}$$

By knowing the air temperature difference across the SAH and the mass flow rate, the useful energy gain can be written as [20]:

$$Q_u = \dot{m}C_P(T_{fo} - T_{fi}) \tag{2}$$

The thermal efficiency of the SAH is the ratio of the useful energy gain to the absorbed energy over a period of time:

$$\eta_{\text{th}} = \frac{Q_u}{Q_i} \tag{3}$$

The thermal efficiency of SC proportional to mass flow rate quantity, i.e., an increased in mass flow rate leads to an increase in thermal efficiency and vice versa. On the other hand, the increased in mass flow rate produce a high-pressure drop which means high energy consuming to pass the air across the SC, it is possible to be equal or larger than useful energy gained by the SC. So, thermo-hydraulic efficiency was the appropriate factor to be considered for comparison purpose. Thermo-hydraulic efficiency of the SC can be estimated as follows [21]:

$$\eta_{th-h} = \frac{Q_u - \frac{P_{mech}}{C_f}}{IA_c} \tag{4}$$

Where C_f is the conversion factor ($C_f = 0.18$), the conversion factor value was recommended by Cortes [21], and P_{mech} is the mechanical power can be estimated by the following equation:

$$P_{mech} = \frac{\dot{m}\Delta P_d}{\rho} \tag{5}$$

Where ΔP_d is the pressure difference across the SC and measured by a manometer.

4. Uncertainties in Experimental Data

Instrumentation accuracy and human error reading caused the uncertainties in the measured data for any parameter. In this study, the relating uncertainties in the air mass flow rate $\delta\dot{m}$ was calculated as described by Refs. [22-23] as follows:

$$\delta\dot{m} = \sqrt{\left(\frac{\partial\dot{m}}{\partial T}\delta T\right)^2 + \left(\frac{\partial\dot{m}}{\partial P}\delta P\right)^2 + \left(\frac{\partial\dot{m}}{\partial V}\delta V\right)^2} \tag{6}$$

Where, $\dot{m}$ is a function of (T, P, V) of the air.
In the same manner, the relating uncertainties in the thermal efficiency η_{th} of the SAH was obtained as follows:

$$\frac{\delta\eta_{th}}{\eta_{th}} = \sqrt{\left(\frac{\delta\dot{m}}{\dot{m}}\right)^2 + \left(\frac{\delta\Delta T}{\Delta T}\right)^2 + \left(\frac{\delta I}{I}\right)^2} \qquad (7)$$

Finally, the uncertainty values of various dependent and independent parameters were listed in Table 1.

Table 1: The uncertainty value of the operational parameters

Parameters	Range	Resolution	Accuracy
Thermocouple type K	-270 - 1260 °C	1 °C	± 1.4 °C
Pyranometer type CMP 22	0 – 4000 W/m^2	∞	± 5 W/m^2
Thermal anemometer	0 – 20 m/s	0.01 m/s	± 0.03 m/s
Uncertainty in measurement			Uncertainty
Temperature, T (°C)			± 1.4
Solar intensity, I (W/m^2)			± 5
Velocity, V (m/s)			± 0.03
Mass flow rate, $\dot{m}$ (kg/s)			± 0.002

5. Results and Discussion

In the present study, the thermal efficiency of the SAH was enhanced due to the fin configurations. Fins were introduced a larger surface area for heat transfer. Besides, metal foam fins with corrugated shaped were increased the residential air time inside SAH duct. That means air cannot be maximized its heat capacity across the SAH without fins. Thereby, this disadvantage could be overcome by using metal foam fins. However, the porosity of metal foam increases the pressure drop across the SAH. So, in this experimental work, the effect of metal foam fins was investigated over various air flow rate ranging between 0.01 m^3/s – 0.05 m^3/s. Measurements and collected data were performed from 9 AM to 4 PM during February, March, and April of 2018.

Solar intensity data were recorded by pyranometer CMP22 in the Iraqi meteorological station in the Ministry of Science and Technology was presented in Fig. 4 for clear sky days in February, March, and April. The solar radiation behavior tends to increase until it reaches its maximum value at noon then starts to decrease again. The temperature difference through the SAH for the three metallic foam fin configurations was presented in Figs. 5 and 6 for the air flow rate of 0.01m^3/s and 0.05 m^3/s. Clearly, the air temperature difference was increased until it reaches its maximum at midday, then it starts to decrease gradually due to the behavior of solar radiation.In general, Fins are used to increase the heat transfer rate from a surface severalfold. Besides, the metal foam was containing a large volume fraction of fluid-filled pores and produce a well mixing between the absorber plate and the air flow. So, the use of metal foam fins will make the heat transfer from the absorber plate to the airflow better than use solid fins. As a result, the temperature difference across the SAH was increased. The corrugated fin configuration showed the highest temperature difference while the longitudinal configuration showed the lowest for all air flow rate range. This belongs to higher turbulence created by the corrugated fins. In addition, corrugated fin configurations introduce more time for air to extract maximum heat from SAH rather than staggered and longitudinal fins. It can be observed that the temperatures difference are changing w.r.t. to the solar intensity variation during the day time. Also, rising the air flow rate leads to decreasing the temperature difference as well as increasing the useful energy gained. The maximum temperature difference for corrugated, staggered, and longitudinal metallic foam fin at an air flow rate of 0.01 m^3/s was 31, 27, and 23°C, respectively.

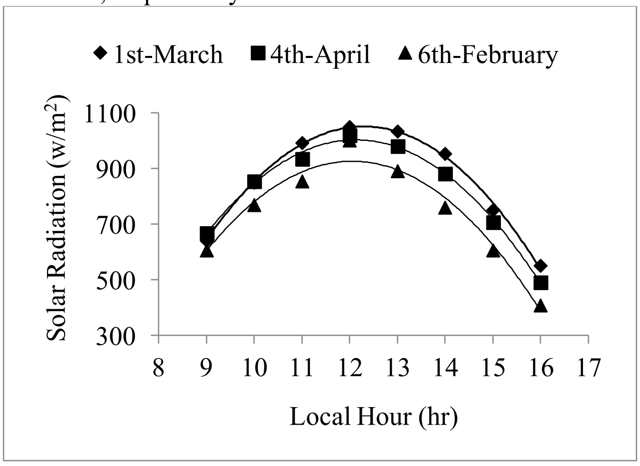

Fig. 4. Solar intensity variation with time for days in February, March, and April of 2018.

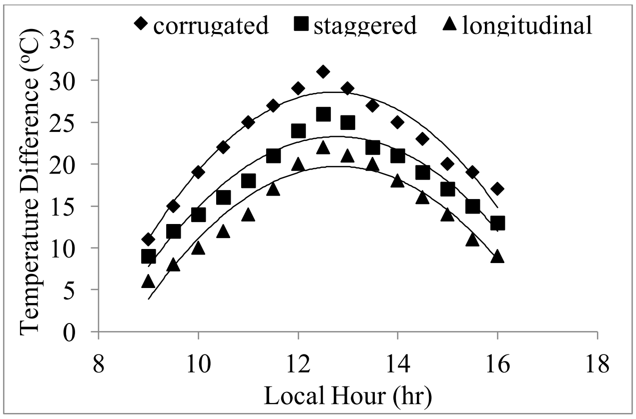

Fig. 5. Measured air temperature difference across SAH for different metal foam fin arrangements at 0.01m^3/s air flow rate.

Fig. 7 summarizes the effect of air flow rate variation on the measured temperature difference across the SAH for all fin configurations. Clearly, the temperature difference was inversely proportional w.r.t. the air flow rate, i.e., increasing the air flow rate causes decreasing the temperature difference due to the same reasons explained in the above paragraph. It can be concluded that, the effect of metal foam on the temperature difference was more significant than solid fin for all air flow rate ranges.

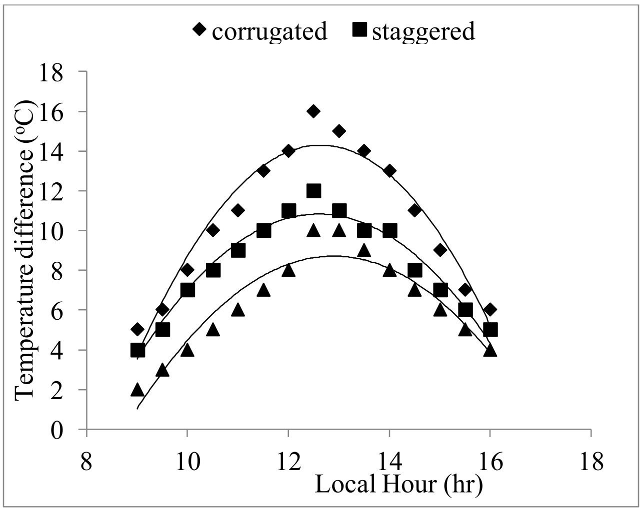

Fig. 6. Measured air temperature difference across SAH for different metal foam fin arrangements at 0.05 m^3/s air flow rate.

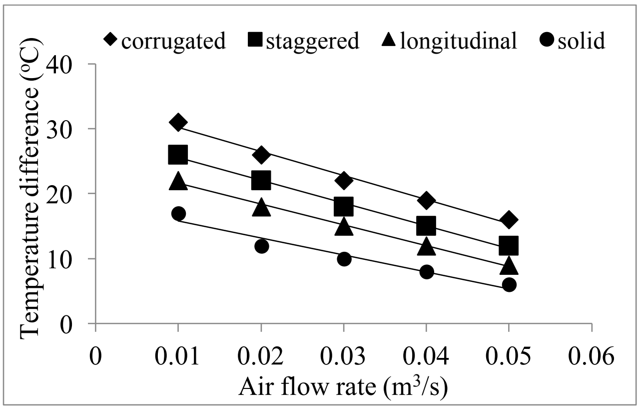

Fig. 7. Maximum air temperature difference for different air flow rates.

Higher thermal efficiency for SC can be achieved by using fins attached to the absorber plate. It is presented a larger surface area for better convective heat transfer; also, it tends to create a turbulent flow inside the SAH. The air temperature difference was measured across the SAH to present the effect of the metal foam fin on the thermal performance. A comparison between solid longitudinal fins with 1 mm thickness and longitudinal metallic foam fins with 5 mm thickness and 15 PPI at 0.01 m^3/s air flow rate depicted in Fig.8. It can be noticed that, the temperature difference across the SAH in the two cases have the same behavior. The obtained results show that the temperature difference for the metal foam fins is higher than the solid fins. The porosity of the metal foam helps the air to penetrate through the fins which means high collisions between air flow and the fin structure. Thereby, air spends more time inside the metal foam fins than the soild fins. So, it is extracted more heat and increasing the thermal efficiency of the SAH. As a result, the use of open cell metal foam fins is more efficient than solid fins in this application. Fig. 9 shows the effect of changing the PPI of metal foam fins on the air temperature difference. The PPI used for comparison were 15 and 20 PPI. The results show that for the same mass flow rate, the metal foam fins with higher PPI exhibited higher temperature difference due to higher heat transfer surface area. In addition, the pore size decreases with increasing the number of PPI. So, the collision time between the air flow and the fin structure will be increased and lead to better temperature difference. In contrast, the consuming pumping power required to push the air across the SAH is increased to overcome the high-pressure drop produces.

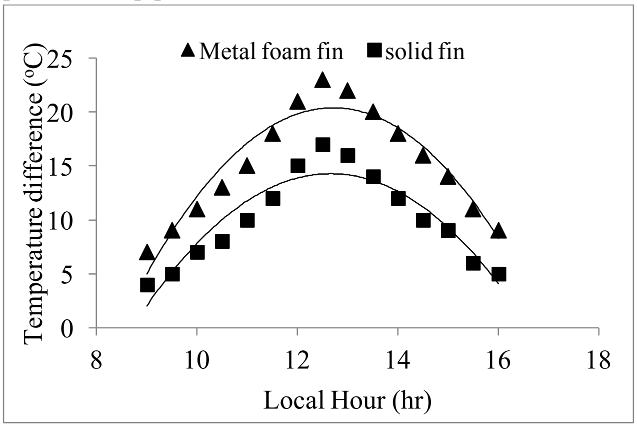

Fig. 8. Measured air temperature difference across SAH for solid longitudinal and longitudinal metal foam fins at 0.01 m^3/s air flow rate.

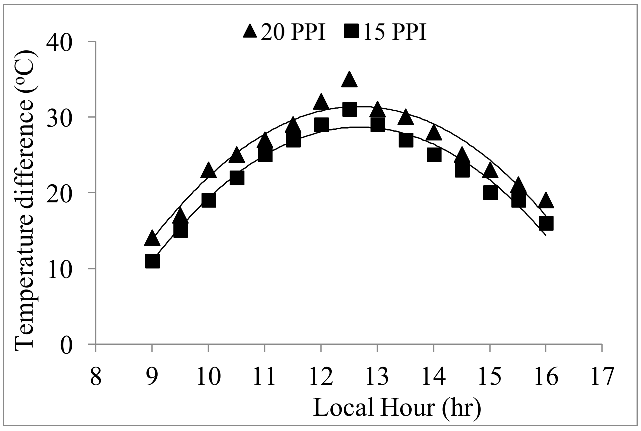

Fig. 9. Measured air temperature difference across SAH for the corrugated arrangement with different PPI at $0.01 m^3/s$ air flow rate.

Fig. 10 depicts the measured values of the useful thermal energy at 0.05 m^3/s air flow rate for different fin configurations. The useful thermal energy of the SAH with metal foam fins is relatively high as compared to the SAH having solid fins. Clearly, the maximum value of the useful thermal energy occurs at mid-day due to the maximum amount of solar radiation. Also, the useful thermal energy values for the corrugated metal foam fins were higher than the values of solid longitudinal fins by 2 – 3 times. This achievement in the useful thermal energy belongs to the better extraction of the available useful thermal energy in the

SAH for the same reasons listed in the above. It can be concluded that the SAH with corrugated metal foam is more thermally efficient than other fin configurations. Thermal efficiency values for all fin configurations were delineated in Fig. 11 for the air flow of 0.05 m^3/s. The behavior of all curves was coincided as compared with the solar radiation curve. The highest value of the thermal efficiency for corrugated, staggered, longitudinal metal foam and solid longitudinal fins are 86 %, 80 %, 75 %, and 53 %, respectively, at an air flow rate of 0.05 m^3/s. Metal foam fins provide air flow sufficient time to exploit the energy from the absorber plate due to the presence of larger surface area for convective heat transfer inside the SAH. Also, metal foam improves the rate of heat transfer by increasing the effective thermal conductivity of the air and making a thinner boundary layer which leads to decrease the thermal resistance. So, it represent the main reasons for the higher values of the thermal efficiency with metal foam fins as compared to solid fins.

In contrast, the effective SAH performance cannot be determined depending on the values of the thermal efficiency due to the high pressure drop across the SAH when using metal foam fins. Consequently, it means much pumping power was required to push the air through the metal foam pores. Therefore, thermo-hydraulic efficiency becomes the correct factor in measuring the SAH effectiveness, i.e., the account of pumping power was taken. The variation of pressure drop as a function of air flow rate for all fin configurations was shown in Fig. 12 for typical test days. It can be noticed that there is a linear relationship between the pressure drops and the air flow rates, i.e., when air flow rate increases lead to increases in the pressure drop because of high friction between the air flow and duct walls. Also, the collisions between air and metal foam boundary lead to more pressure drop in the SAH. Thus, the maximum pressure drop value was 190.7 Pa in the SAH that used corrugated metal foam fins whereas; minimum value was 127.5 Pa for longitudinal metal foam fins at the maximum air flow rate. This feature represents an essential disadvantage of the metal foam due to the high energy consumption during pumping air across the SAH.

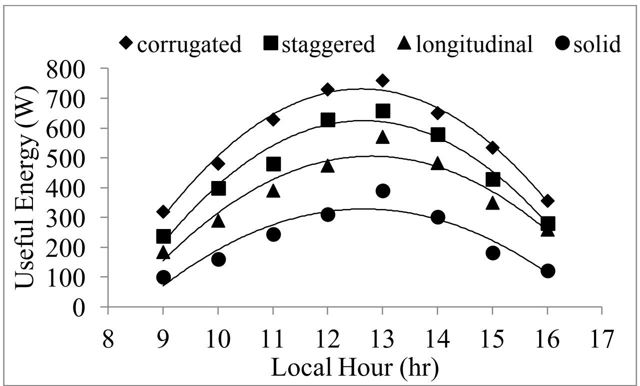

Fig. 10. Variation of useful energy gained with time for all arrangements at an air flow rate of 0.05 m^3/s.

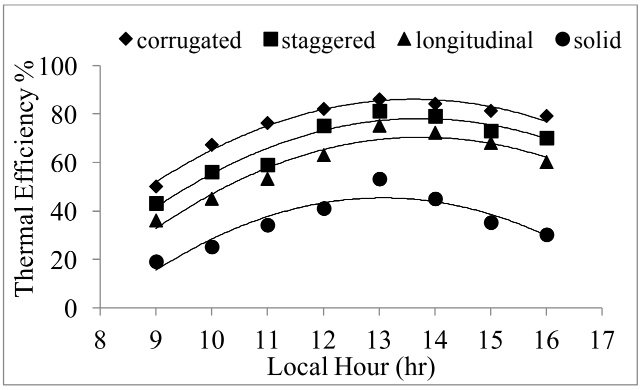

Fig. 11. Variation of thermal efficiency with time for all arrangements at an air flow rate of 0.05 m^3/s.

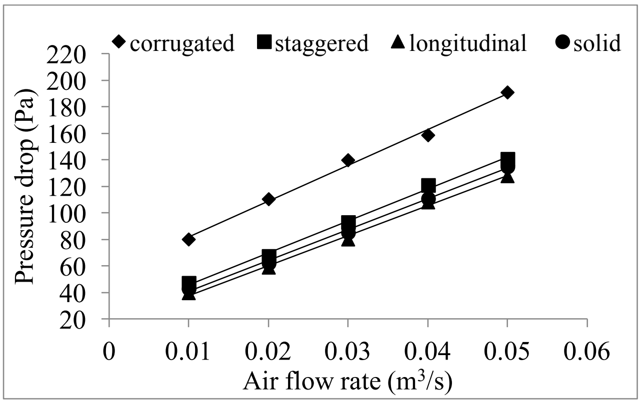

Fig. 12. Measured pressure drops as a function of air flow rates for all fin configurations.

Fig. 13 depicts the values of thermo-hydraulic efficiency as a function of air flow rate for all fin configurations. The maximum value of thermo-hydraulic efficiency was 79 % for corrugated fins at 0.05 m^3/s while; the minimum value was 44 % for solid fins at 0.04 m^3/s. Clearly, despite high-pressure drop occurs in corrugated fins it still has higher thermo-hydraulic efficiency.

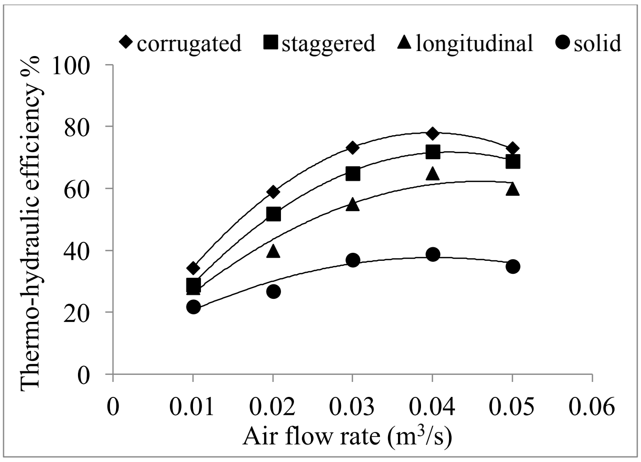

Fig. 13. Variation of thermo-hydraulic efficiency with time for all fin arrangements.

6. Conclusions

This experimental study investigates the effect of using different metal foam and solid fin configurations attached to the back surface of the absorber plate. The SAH was operated for the air flow rate varying from 0.01 m^3/s to 0.05 m^3/s. Useful energy, Thermal efficiency, and thermo-hydraulic efficiency were obtained by measured average air temperatures across the SAH. Based on the present experimental tests, the following conclusions can be drawn:

1. The highest value of the thermal and thermo-hydraulic efficiencies for corrugated, metal foam fins are 86 %, and 79 %, respectively, at an air flow rate of 0.05 m^3/s, i.e., the SAH with corrugated metal foam is more thermally efficient than other fin configurations.
2. Increasing the air flow rate leads to decreasing the temperature difference as well as increasing the useful energy gained. The maximum temperature difference for corrugated, staggered, longitudinal metallic foam, and solid longitudinal fins at an air flow rate of 0.01 m^3/s was 31, 27, 23, and 17℃, respectively.
3. Metal foam fins with higher PPI exhibited higher temperature difference due to higher heat transfer surface area.
4. The Metal foam fins showed a better performance than the solid fins for all air flow rates.

Nomenclature

A_c	Area of absorber plate, m^2
C_f	Conversion factor
C_p	Specific heat of air at constant pressure, J/kg K
I	Solar radiation intensity, W/m^2
$\dot{m}$	Air mass flow rate, kg/s
P_{mech}	Mechanical power, W
ΔP_d	Pressure drop, Pa
Q_i	Absorbed energy, W
Q_u	Useful energy, W
T_{fi}	Inlet air temperature, ^oC
T_{fo}	Outlet air temperature, ^oC
ΔT	Air temperature difference ($T_{fo} - T_{fi}$), ^oC
V	Air velocity, m/s
δ	Uncertainty in measurements
η_{th}	Thermal efficiency, %
$\eta_{th\text{-}h}$	Thermo-hydraulic efficiency, %
ρ	Air density, kg/m^3

References

[1] F. Jamadi , M. Arabpour, M. Abdolzadeh, Performance Comparison of Parabolic and Flat Plate Solar Collectors Utilizing in the Heating System of a Room-An Experimental Investigation, International Journal of Renewable Energy Research, Vol.7, No.4: 1836-1849, 2017

[2] A. Al-Ghasem, G. Tashtoush and M. Aladeemy, "Experimental study of tracking 2-D Compound Parabolic Concentrator (CPC) with flat plate absorber," 2013 International Conference on Renewable Energy Research and Applications (ICRERA), Madrid, 2013, pp. 779-782.

[3] A. H. Işik, Ş. Erden and M. İmeryüz, "Design of the solar energy system in ITU faculty of electric and electronics," 2015 International Conference on Renewable Energy Research and Applications (ICRERA), Palermo, 2015, pp. 867-871.

[4] A.E. Kabeel, M.H. Hamed, Z.M. Omara, and A.W. Kandeal, “Solar air heaters: Design configurations, improvement methods and applications–A detailed review”. Renewable and Sustainable Energy Reviews, 70, pp.1189-1206, 2017.

[5] M. Mahdi and A. Gaddoa, “Outdoor Testing of a Zig-Zag Solar Air heater with and without Artificial Roughness on Absorber Plate”, Journal of Engineering, vol. 25, no. 4, pp. 1-17, Apr. 2019.

[6] S. Simms and J. Dorville, "Thermal performance of a hybrid photovoltaic-thermal collector with a modified absorber," 2015 International Conference on Renewable Energy Research and Applications (ICRERA), Palermo, 2015, pp. 600-605.

[7] A.A. Farhan and H. A. Sahi, “Energy Analysis of Solar Collector With perforated Absorber Plate”, Journal of Engineering, 23(9), pp. 89-102, 2017.

[8] K. Mohammadi, and M. Sabzpooshani, “Comprehensive performance evaluation and parametric studies of single pass solar air heater with fins and baffles attached over the absorber plate”. Energy, 57, 741-750, 2013.

[9] H. M. Yeh, “Upward-type flat-plate solar air heaters attached with fins and operated by an internal recycling for improved performance”. Journal of the Taiwan Institute of Chemical Engineers, 43(2), 235-240, 2012.

[10] N. Moummi, S. Youcef-Ali, A. Moummi, and J.Y. Desmons, “Energy analysis of a solar air collector with rows of fins”. Renewable Energy, 29(13), 2053-2064, 2004.

[11] K. Sopian, M.A. Alghoul, E. M. Alfegi, M. Y. Sulaiman, and E.A. Musa, “Evaluation of thermal efficiency of double-pass solar collector with porous–nonporous media”. Renewable Energy, 34(3), 640-645, 2009.

[12] R. Kumar, and P. Chand, “Performance enhancement of solar air heater using herringbone corrugated fins”. Energy, 127, 271-279, 2017.

[13] H. Hassan, and S. Abo-Elfadl, “Experimental study on the performance of double pass and two inlet ports solar air heater (SAH) at different configurations of the

absorber plate”. Renewable Energy, 116, 728-740, 2018.

[14] M. H. Ahmed, A. Giaconia and A. M. A. Amin, "Effect of solar collector type on the absorption system performance," 2017 IEEE 6th International Conference on Renewable Energy Research and Applications (ICRERA), San Diego, CA, 2017, pp. 304-309.

[15] I. E. Haber, "Energy transport modeling of PV/T collectors," 2015 International Conference on Renewable Energy Research and Applications (ICRERA), Palermo, 2015, pp. 1615-1617.

[16] J. Chen, D. Yang, J. Jiang, A. Ma, and D. Song, “Research progress of phase change materials (PCMs) embedded with metal foam (a review)”. Procedia Materials Science, 4, 389-394, 2014.

[17] Z. Chen, M. Gu, D. Peng “Heat transfer performance analysis of a solar flat-plate collector with an integrated metal foam porous structure filled with paraffin”. Applied Thermal Engineering, 30:1967–73, 2010.

[18] A. O. Dissa, S. Ouoba, D. Bathiebo, J. Koulidiati “A study of a solar air collector with a mixed porous and non-porous composite absorber”, Solar Energy, 129:156–74, 2016.

[19] Saman Rashidi, Javad Abolfazli Esfahani, Abbas Rashidi,”A review on the applications of porous materials in solar energy systems”, Renewable and Sustainable Energy Reviews 73: 1198–1210, 2017.

[20] J. A. Duffie, and W. A. Beckman, “Solar engineering of thermal processes”. 4th ed., John Wiley & Sons 2013.

[21] A.Cortes, and R. Piacentini, “Improvement of the efficiency of a bare solar collector by means of turbulence promoters”. Applied Energy, 36(4), 253-261, 1990.

[22] J.P. Holman. “Experimental Methods for Engineers”, McGraw-Hill, New York, 1989.

[23] R.J. Moffat, “Describing the uncertainties in experimental results”, Experimental Thermal and Fluid Science, 1 (1) 3–17, 1988.